Seismic Observations on Piled Raft Foundation with Ground Improvement Supporting a Base-Isolated Building

Junji HAMADA, Tomohiro TANIKAWA, Sadatomo ONIMARU & Kiyoshi YAMASHITA
Research & Development Institute, Takenaka Corporation, Japan

SUMMARY:
The purpose of this study is to clarify the seismic performance of piled raft foundations with ground improvement based on seismic observation records. The monitored building, which is a twelve-story base-isolated building, is located on loose silty sand underlain by soft cohesive soil in Tokyo, Japan. On March 11, 2011, the 2011 off the Pacific coast of Tohoku Earthquake struck the building site, the seismic response of the soil-foundation-structure system was successfully recorded during the earthquake. Axial force and bending moment of two piles, earth pressure and pore-water pressure beneath the raft, and accelerations of the ground and structure were measured. It was found that the peak acceleration reduction of input motion caused by ground improvement. The sectional forces of piles at the pile head and at intermediate depth were almost same behavior. The bending moments increased during large ground deformation.

Keywords: The 2011 off the Pacific coast of Tohoku Earthquake, Pild raft foundation, Seismic observation, Pile

1. INTRODUCTION

Piled raft foundations are recognized as a considerable economy system without compromising the safety and performance of the foundation (Poulos, 2001; Mandolini et al., 2005). A lot of experimental and analytical studies for piled raft foundations have been conducted to investigate the settlement behavior and the load-sharing between raft and piles for vertical loading (Katzenbach et al., 2000; Yamashita et al., 2011a). It is necessary to develop a seismic design concept for the piled raft foundations especially in highly active seismic areas such as Japan. In the last decade, shaking table tests and static lateral loading tests using centrifuge model or large scale model (Watanabe et al., 2001; Horikoshi et al., 2003; Matsumoto et al., 2004; Katzenbach & Turek, 2005; Matsumoto et al., 2010; Hamada et al., 2011), analytical studies (Kitiyodom & Matsumoto, 2003; Hamada et al., 2009) have been carried out. Mendoza et al. (2000) reported about static and seismic behaviour of a piled-box foundation supporting an urban bridge in Mexico City clay, i.e. the response of the soil-foundation system were recorded during the occurrence of two seismic events in 1997 where the maximum horizontal acceleration of the foundation was 0.31 m/s^2. However, only a few case histories exist on the monitoring the soil-pile-structure interaction behavior during earthquakes.

The purpose of this study is to clarify the seismic performance of piled raft foundations based on seismic observation records. The monitored building, which is a twelve-story base-isolated building, is located on loose silty sand underlain by soft cohesive soil in Tokyo, Japan. A piled raft with ground improvement was employed to cope with the liquefiable sand as well as to improve the bearing capacity of the raft foundation. On March 11, 2011, the 2011 off the Pacific coast of Tohoku Earthquake struck the building site, the seismic response of the soil-foundation-structure system was successfully recorded during the earthquake. Axial force and bending moment of two piles, earth pressure and pore-water pressure beneath the raft, and accelerations of the ground and structure were measured. In this paper, the characteristics of observed seismic motion of the ground and the building as well as the sectional forces of the piles will be discussed.

2. MONITORED BUILDING AND SOIL CONDITIONS

Seismic monitored building is the twelve-story residential building located in Tokyo, Japan. The building is a reinforced concrete structure, 38.7m in height, 30.05m and 33.25m in width, with a base isolation system of laminated rubber bearings. Figure 1 shows a schematic view of the building and the foundation with typical soil profiles.

The soil profile down to a depth of 7 m is made of fill and loose silty sand, and from 7 m to 44 m, there lie very-soft to medium silty clay strata. The silty clay between depths of 7 m to 15.5 m is slightly overconsolidated with an overconsolidated ratio (OCR) of about 1.5 and the silty clay between depths of 15.5 m to 44 m is overconsilidated with OCR of 2.0 or higher. The subsoil consists of an alluvial stratum to a depth of 44 m, underlain by a diluvial sand and gravel layer of SPT N-values of 60 or higher. The ground water table appears approximately 1.8 m below the ground surface. The shear wave velocities derived from a P-S logging system were 110 to 220 m/s between depths of 4.8m and 43 m, and 410 to 610 m/s in the dense sand and gravel layers below a depth of 48 m.

The piled raft foundation design was described in a previous paper (Yamashita et al., 2011b). The average contact pressure over the raft was 199 kPa. To improve the bearing capacity of the subsoil beneath the raft, as well as to cope with the liquefiable silty sand, the grid-form deep cement mixing walls were embedded in the overconsolidated silty clay with undrained shear strength of 75 kPa below a depth of 16 m. Consequently, a piled raft consisting of sixteen 45-m long bored precast concrete piles with diameter of 0.8 to 1.2 m (SC piles in top portion, PHC piles in other portion) were employed.

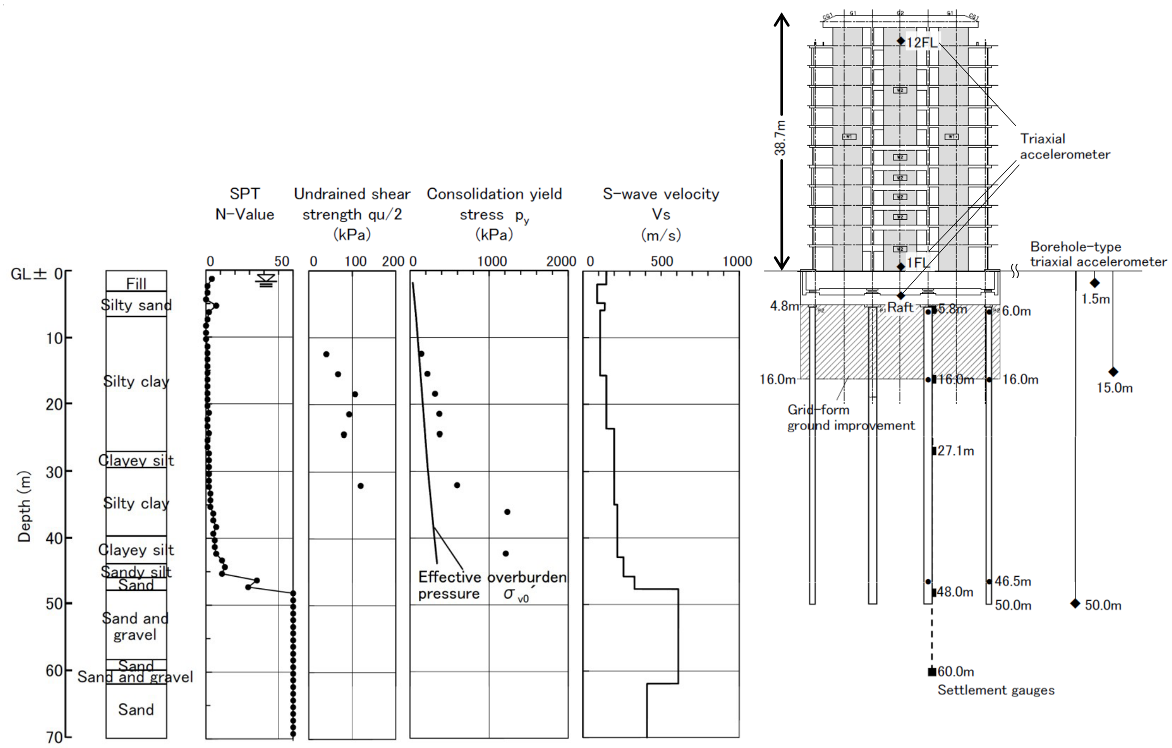

Figure 1. Schematic view of the building and foundation with soil profile

3. INSTRUMENTATION

The locations of the monitoring devices are shown in Figures 1 and 2. As for the seismic observation, the NS, EW and UD accelerations of the free-field ground were measured by the vertical array consisted of borehole-type triaxial servo accelerometers installed at depth of 1.5 m, 15.0 m and 50.0 m below the ground surface and those of the building on the raft, the first and the twelfth floors were recorded by triaxial servo accelerometers. The horizontal components of the triaxial accelerometers were oriented to the longitudinal direction and the transverse direction of the building which are almost identical with north-south direction and east-west direction, respectively, as shown in Figure 2. In this paper, the longitudinal direction of the building is called NS-direction and the transverse direction of the building is called EW-direction. The triggering acceleration is 0.004 m/s^2 at 50.0 m below the ground surface and the sampling rate is employed at 100 Hz.

The axial forces and bending moments of two piles, the contact earth pressures between the raft and the soil as well as the pore-water pressure beneath the raft were also measured during the earthquake in common starting time with the accelerometers. The piles, 5B and 7B, were provided with a couple of LVDT-type strain gauges at depths of 6.0 m (pile head), 16.0 m and 46.5 m. Measuring system is consisted of IC Card Data Logger, Dynamic Amplifier, Power Unit and UPS shown in Photo 1 and Table 1.

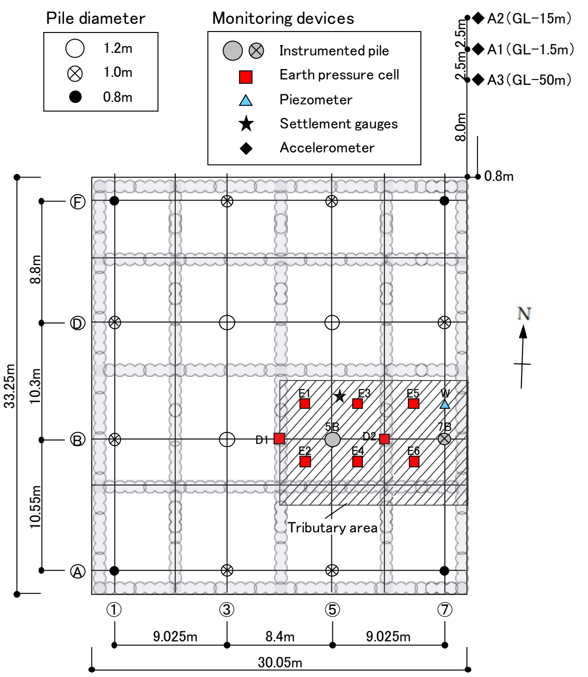

Figure 2. Layout of piles and grid-form deep cement mixing walls with locations of monitoring devices

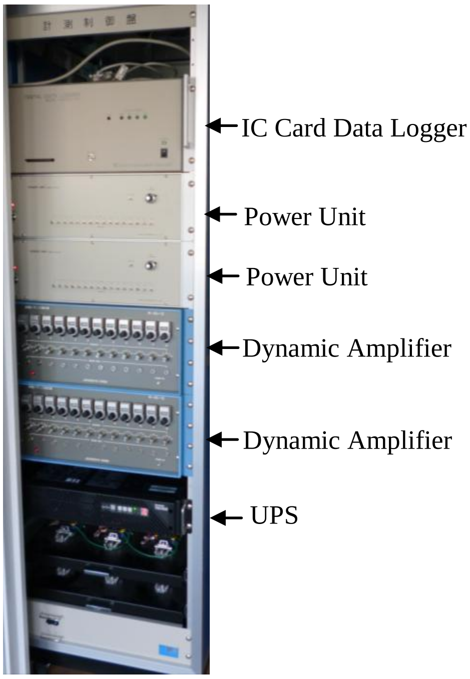

Photo 1. Layout of measuring system

Table 1. Property of measuring devices

Device	Property
IC Card Data Logger	AD converter 24bit, Sampling 100Hz
Servo Accelerometer (structure, ground)	Tri-axis, Full scale:±2000gal
Dynamic Amplifier	LVDT. Frequency Response:20Hz
Strain gauge	LVDT
Earth pressure cell improved soil intact soil	LVDT Capacity:500kPa Capacity:200kPa
Piezometer	LVDT, Capacity:100kPa
Settlement gauge	LVDT

4. SEISMIC RESPONSE OF PILED RAFT FOUNDATION AND SURPERSTRUCTURE

The 2011 off the Pacific coast of Tohoku Earthquake struck the building site. The distance from the epicenter to the building site was about 380 km. The seismic responses of the soil-structure system were successfully recorded (Yamashita et al., 2012).

4.1. Observed Seismic Response of Foundation and Surperstructure

4.1.1. Accelerations of the ground and the structure

Figure 3 shows the time histories of the EW acceleration (the transverse direction of the building) of the ground and the structure. Horizontal directions of the borehole-type accelerometers set in the ground were examined and modified using long-period component of observed seismic accelerations. The peak horizontal ground acceleration of 1.748 m/s^2 was observed near the ground surface. Figure 4 shows the profiles of the maximum amplitudes of the accelerations of the ground and structures.

The peak ground acceleration in EW direction near the ground surface is 3.2 times amplified from the depth of 50.0 m. The peak acceleration in EW direction of the first floor was 0.527 m/s^2 which was reduced to 52 % from that at the raft of 1.002 m/s^2 by the base-isolation system. And also, the peak acceleration in EW direction of the raft was reduced to 57 % from that at the ground surface of 1.748 m/s^2 by the kinematic soil-foundation interaction.

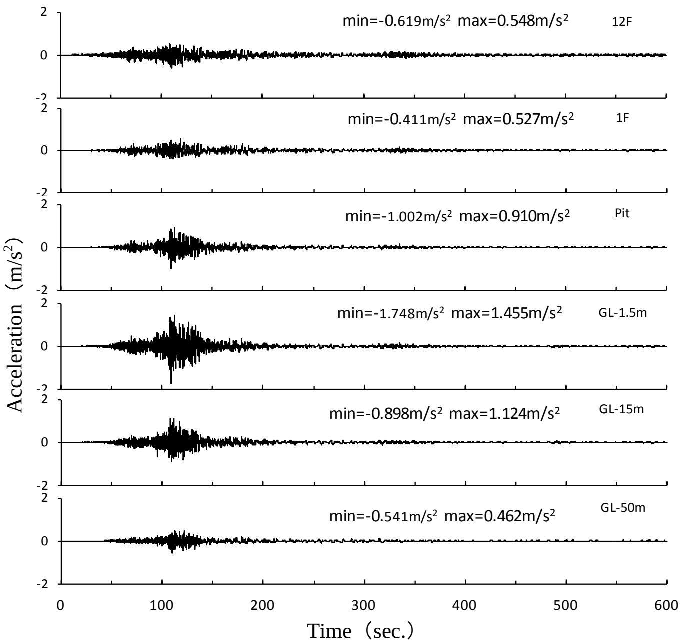

Figure 3. Time histories of EW accelerations of the ground and the structure

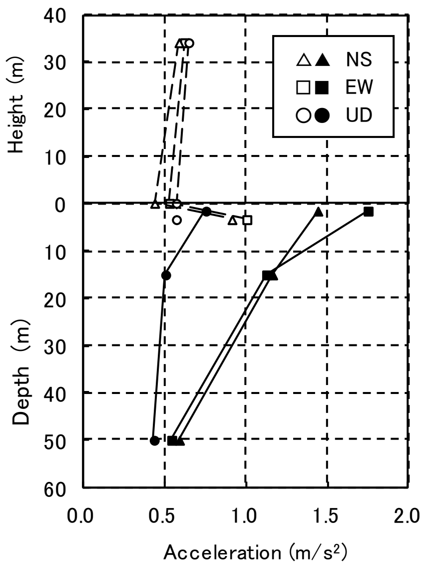

Figure 4. Maximum amplitude of accelerations of the ground and structure

Figure 5 shows the Fourier spectra of the accelerations of the ground and structures, which were smoothed by 0.05 Hz Parzen wondow. As to the accelerations near the ground surface, a component of the period around 1.0 second was predominant, and the responses of the superstructures, first and twelfth floors, were amplified around 3.5 second. The natural period of the base-isolation system in the horizontal directions of the earthquake was found to be approximately 3.5 second.

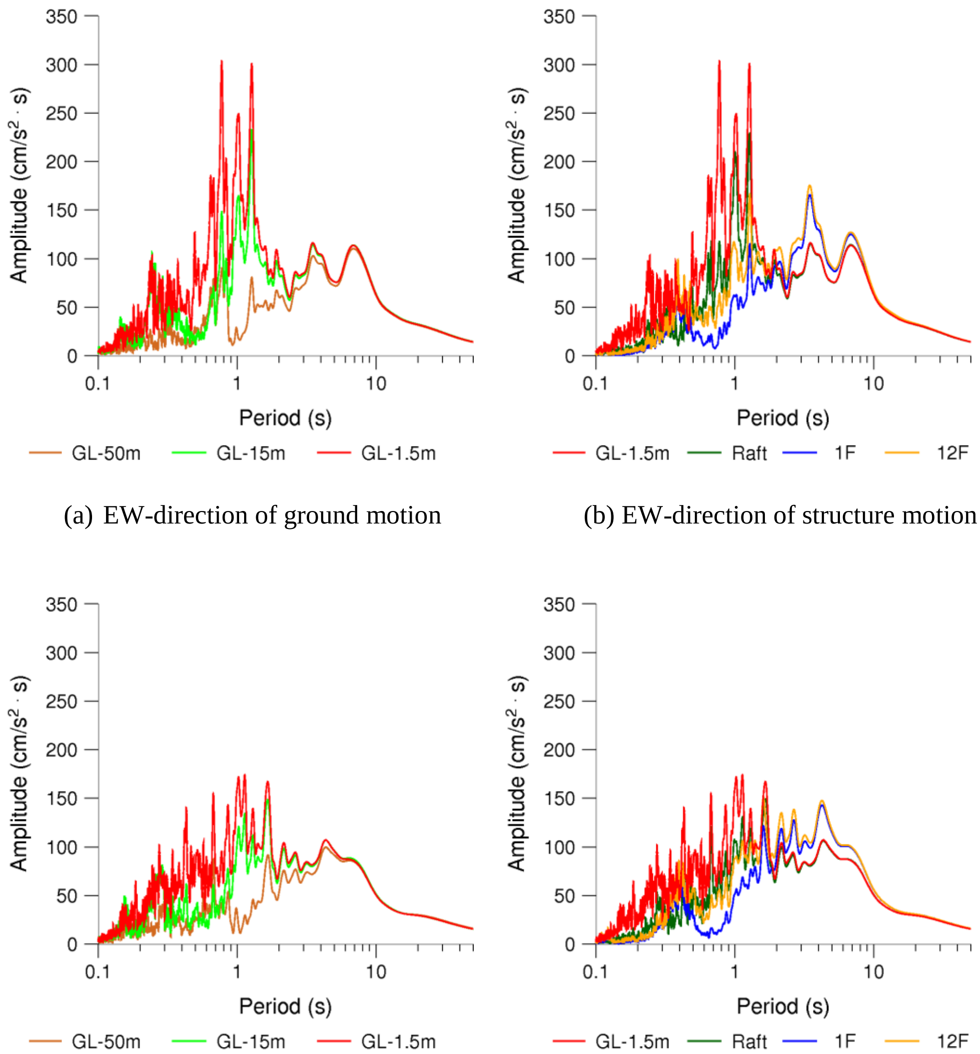

(a) EW-direction of ground motion (b) EW-direction of structure motion

(c) NS-direction of ground motion (d) NS-direction of structure motion

Figure 5. Fourier spectra of the ground and structure accelerations

4.1.2. Sectional forces of piles

Figures 6 and 7 show the time histories of the incremental sectional forces of pile 5B and 7B, respectively. The sectional forces at near the pile head, 6 m below the ground surface (that means 1.2 m below the pile head), were compared with those at intermediate depth, 16 m below the ground surface as well as 46.5m below the ground surface (in case of 7B) magnified from 100 to 120 seconds. Table 2 shows the observed incremental maximum values of the sectional forces of piles 5B and 7B. The positive and negative values of the incremental axial forces mean compression and tension, respectively.

The axial forces at intermediate depth of 16 m below the ground surface where is lower end of grid-form deep cement mixing walls behaved similarly those at the pile head. And also, the bending moments at lower end of grid-form deep cement mixing walls behaved in same phase with those at the pile head. The positive peak axial forces of pile 7B of 1.0m diameter were about 690kN at pile head and 760kN at intermediate depth, respectively and the peak bending moments of the pile were about 210kNm at pile head and 155kNm at intermediate depth, respectively. It is estimated that the frictional resistances around the piles enclosed by the grid-form walls were small and also the bending moments at pile head were reduced by the grid-form walls whereas those at intermediate depth, at lower end of the grid-form walls, behaved similar to those at pile head.

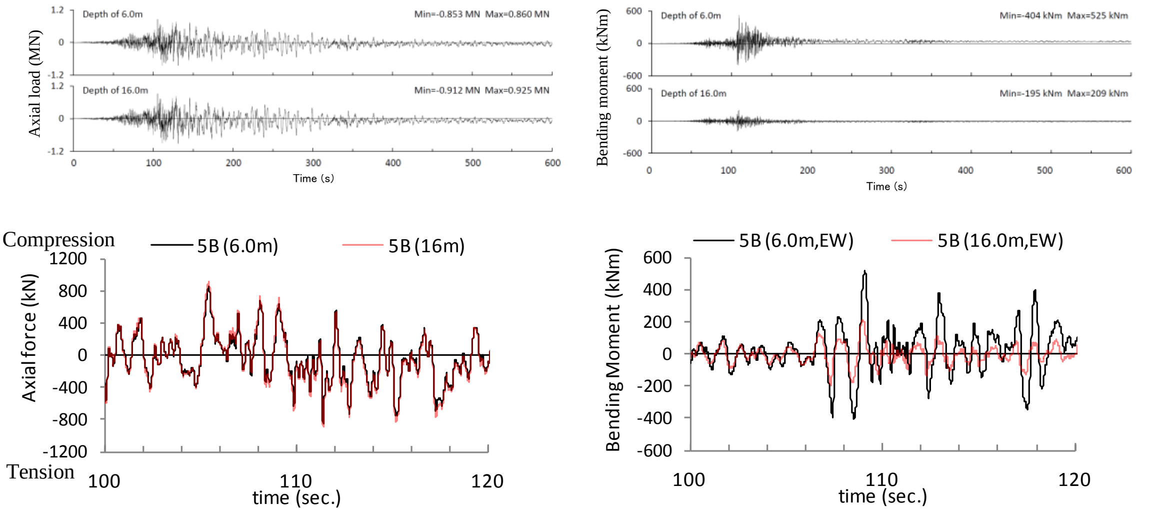

(a) Axial forces (b) Bending moments

Figure 6. Time histories of the incremental sectional forces of pile 5B

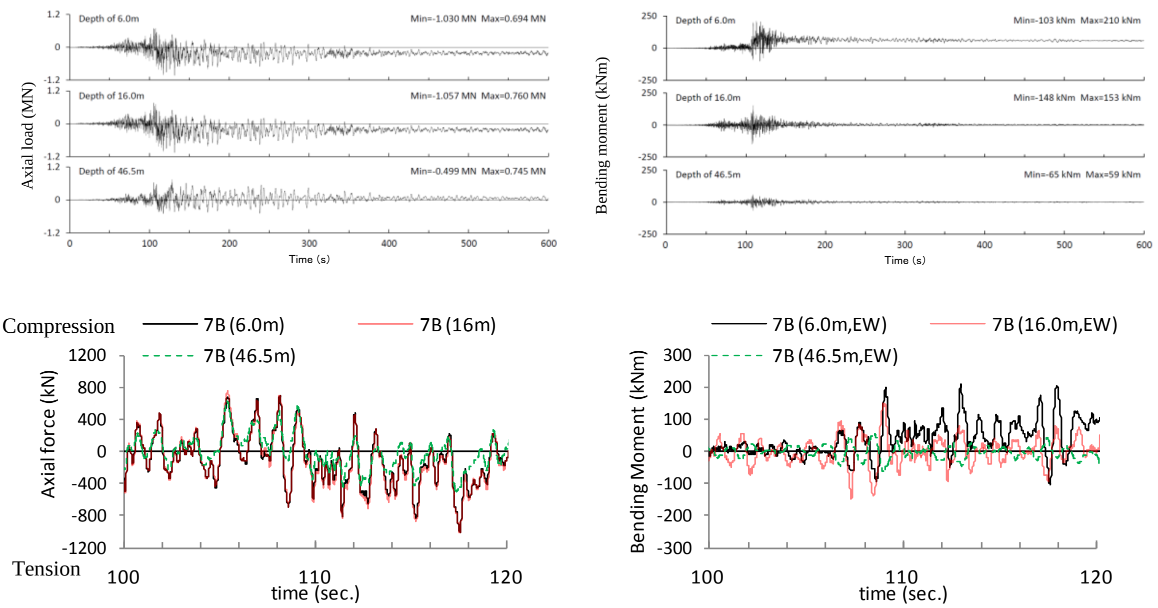

(b) Axial forces (b) Bending moments

Figure 7. Time histories of the incremental sectional forces of pile 7B

Table 2. Maximum incremental sectional forces of piles

Bending Moment	EW-direction				NS-direction				absolute
kNm	min	time (s)	max	time (s)	min	time (s)	max	time (s)	maximun
7B (6.0m)	-102.9	58.8	210.3	56.5	-79.4	55.9	84.6	59.9	211.7
7B (16.0m)	-148.2	53.7	153.4	54.5					
7B (46.5m)	-65.1	54.5	59.0	54.2					
5B (6.0m)	-403.8	54.3	525.4	54.5	-216.1	58.1	184.3	57.3	528.9
5B (16.0m)	-195.3	53.7	208.6	54.5					

Axial Force	Tension		Compression	
kN	min	time (s)	max	time (s)
7B (6.0m)	-1030.4	131.48	693.6	108.13
7B (16m)	-1057.2	131.48	760.0	105.39
7B (46.5m)	-498.5	117.36	745.4	128.52
5B (6.0m)	-853.1	131.44	859.6	105.39
5B (16m)	-912.5	131.43	924.8	105.39

4.1.3.Contact earth pressure and water pressure beneath the raft

Figure 8 shows the time histories of the incremental contact pressures between the raft and the improved soil and those between the raft and the intact soil. The amplitudes of the incremental contact pressures between the raft and the improved soil were significantly larger than those between the raft and the intact soil.

The records of the earth pressure cells from E1 to E6 and D2, except for D1, were suddenly increased after 107 to 109 seconds and residual stresses were occurred, which is generally consistent with the records of the axial loads on pile 7B as shown in Figure 7.

The excess pore-water pressure induced during the earthquake was considerably smaller than the contact pressures between the raft and the intact soil. The excess pore-water pressure was gradually increased 1.2kPa one hour after the start of the event as shown in Figure 9. The aftershock of M7.6 occurred at 29 minutes after the start of the events was recorded, and excess water pressure has been slightly increasing.

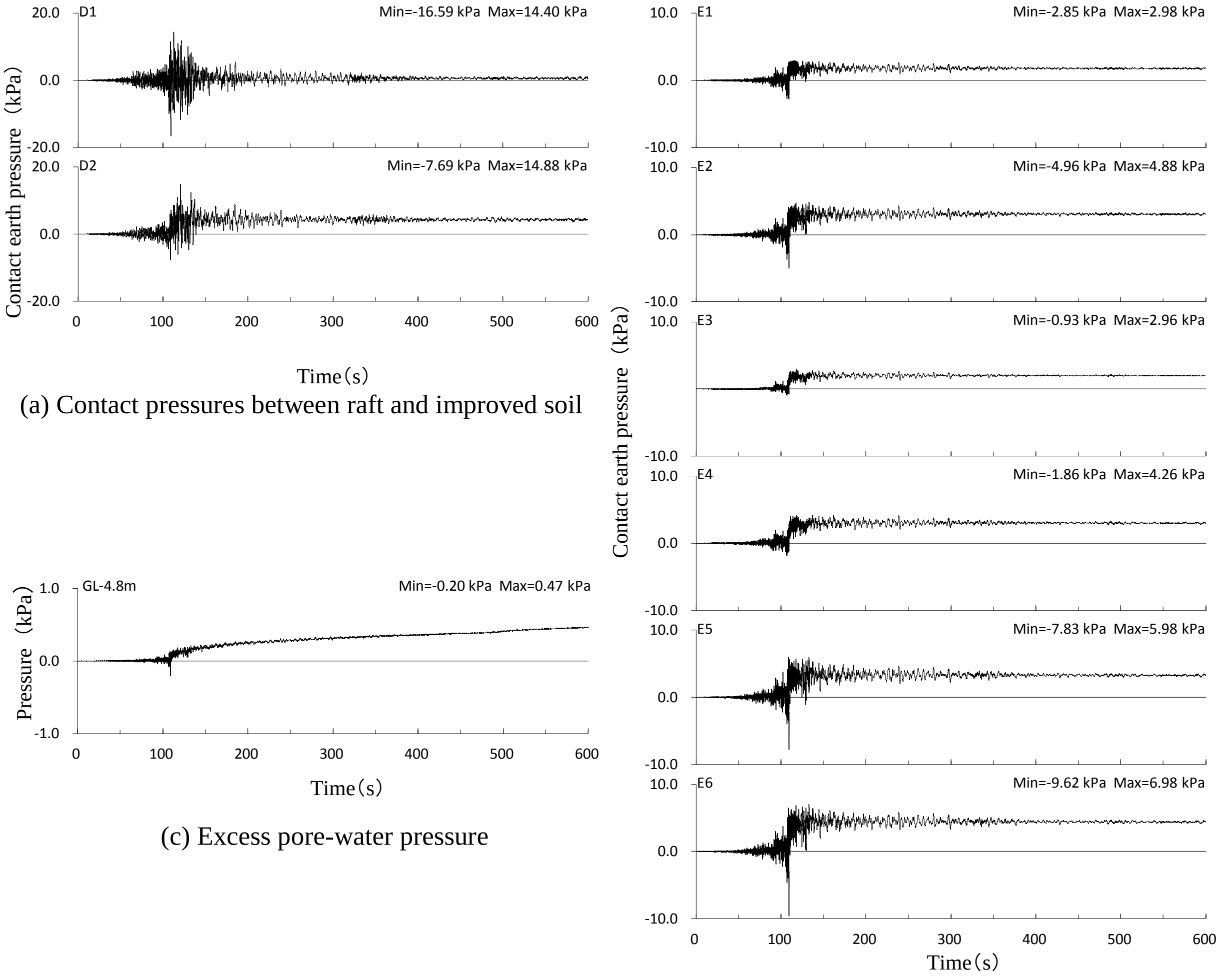

(a) Contact pressures between raft and improved soil

(c) Excess pore-water pressure

(b) Contact pressures between raft and intact soil

Figure 8. Time histories of contact pressures and excess pore-water pressure

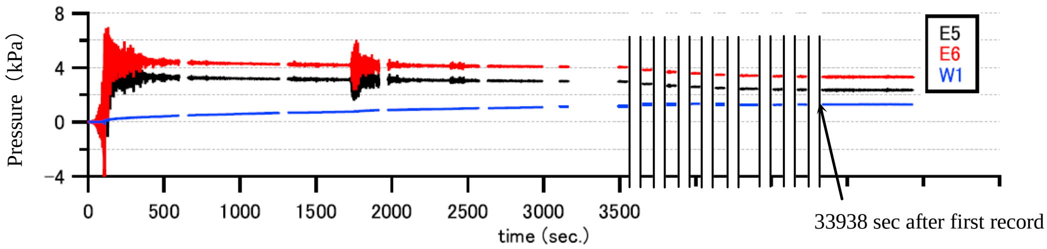

Figure 9. Long term histories of excess pore-water pressure and earth pressures

4.2. Effects of inertial force and ground displacement on bending moment of piles

Figure 10 shows the horizontal displacements near the ground surface relative to those at a depth of 50 m versus the incremental bending moments at the pile head. The horizontal displacements were calculated by the integration of acceleration records, where components of the period longer than 20 second and shorter than 0.05 second were cut off. The bending moments at the pile head tend to increase with the increase in the relative horizontal displacements for both piles 5B and 7B.

Figure 11 shows the inertial force of building versus the incremental bending moments at the pile head. The inertial force of building was estimated from multiplying the building weight by observed accelerations on the raft, the first and the twelfth floors. The weights of the superstructure above the isolators and the substructure under the isolators are 152MN and 41MN, respectively. Figure 12 shows the inertial force of building versus the incremental bending moments at the pile head from 200 to 300 seconds which range is relatively minor ground surface displacement. However the bending moments at the pile head tend to increase with the increase in the inertial force of building, the effect of the inertial force for the bending moment of the pile head was not significant comparing with the ground deformation. The points of Time A and B in Figures 10 and 11 correspond to times shown in Figures 13, 14 and 15.

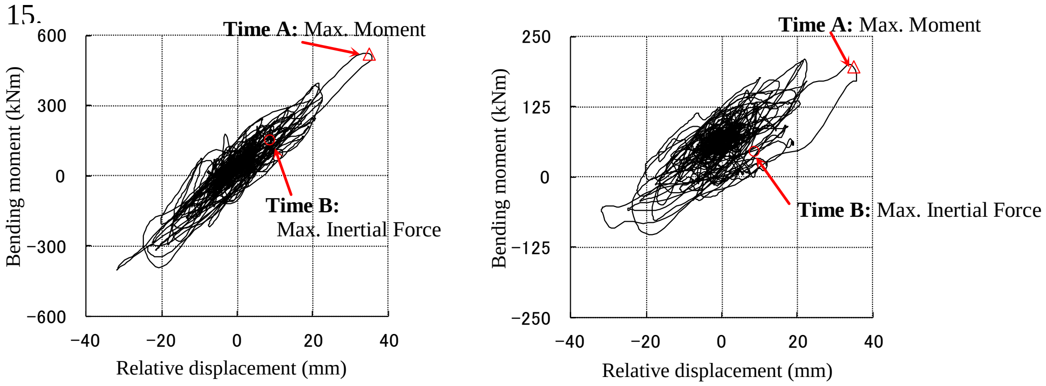

(a) Pile 5B (EW) (b) Pile 7B (EW)

Figure 10. Relative ground displacements vs. bending moments at pile head

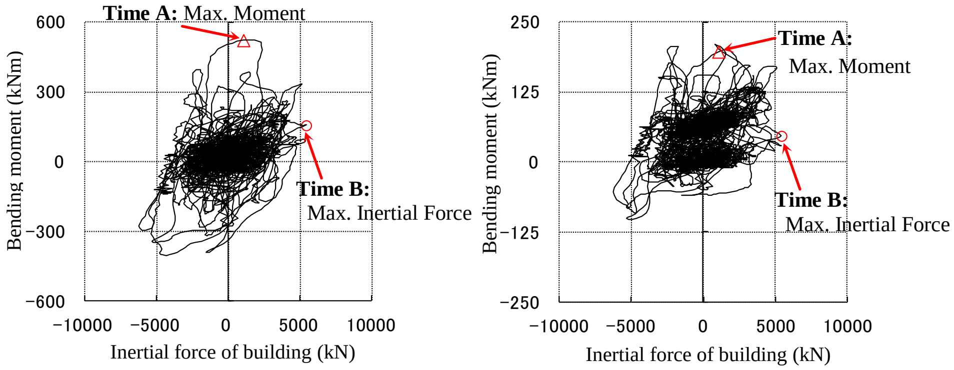

(a) Pile 5B (EW) (b) Pile 7B (EW)

Figure 11. Inertial forces vs. bending moments at pile head

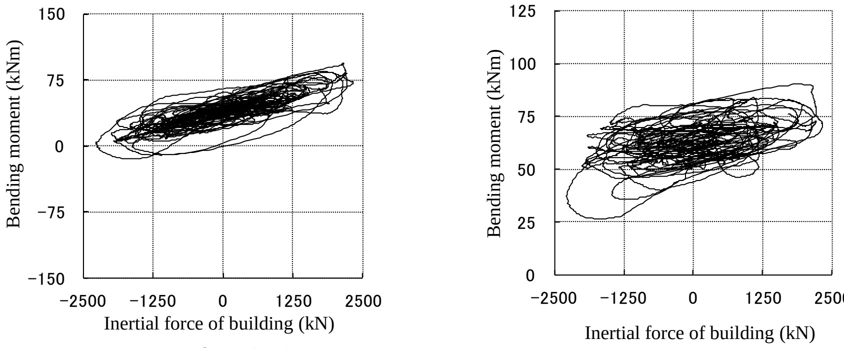

(a) Pile 5B (EW) (b) Pile 7B (EW)

Figure 12. Inertial forces vs. bending moments at pile head (200 to 300 seconds)

Figure 13 shows the profiles of the accelerations, the relative displacements of the ground and structure, and bending moments in EW direction when EW incremental bending moment at the pile head of pile 5B was maximum shown in Table 2. Figure 14 shows those profiles when EW inertial force of building was maximum value. Figure 15 shows the time histories of the inertial force of building, the relative displacements, the sectional forces and earth pressures from 100 to 120 seconds. Dashed lines correspond to times of Figures 13 and 14. It was found that the bending moments at the pile head and those at the intermediate depth increased during large deformation of the ground in spite that the inertial force of building was not significant.

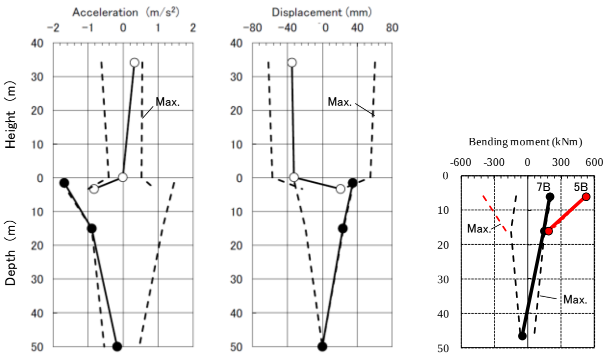

(a)Accelerations (b) Displacements (c) Bending moments

Figure 13. Profiles of accelerations, displacements and bending moments in EW direction (Maximum bending moment of 5B, Time A:t=109.07 sec.)

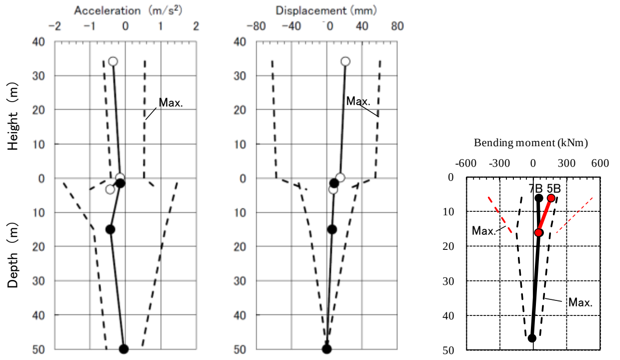

(a)Accelerations (b) Displacements (c) Bending moments

Figure 14. Profiles of accelerations, displacements and bending moments in EW direction (Maximum inertial force, Time B: t=106.96 sec.)

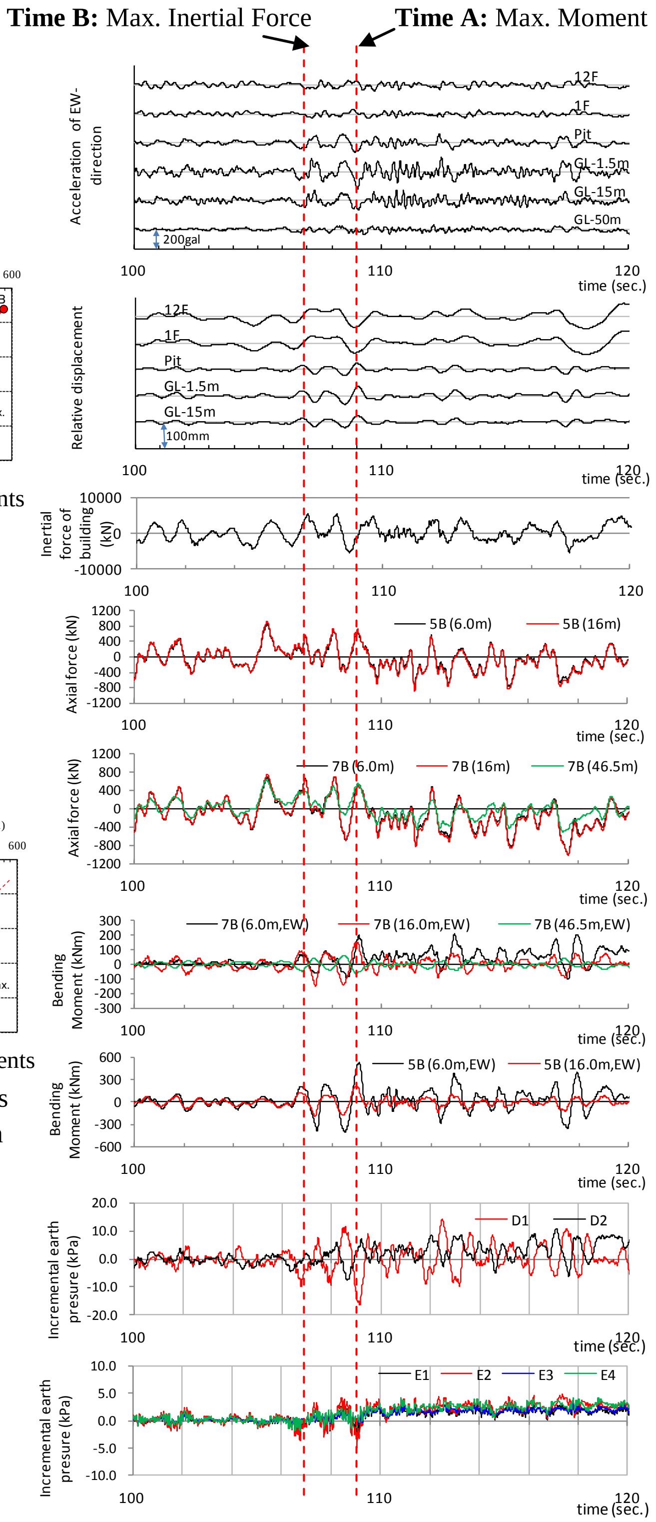

Figure 15. Time histories of inertial force of building, relative displacements, sectional forces and earth pressures

6. CONCLUSIONS

It was found that the horizontal acceleration, peak of 0.62 m/s^2, of the superstructure was significantly reduced compared to that on the raft, peak of 1.00 m/s^2, by the base isolation system. And also, the peak acceleration on the raft was about 60 percent of that of the ground surface of 1.75 m/s^2 in the site of the building. It is considered that reduction of input motion could be caused by ground improvement.

The sectional forces of piles at near the pile head and at intermediate depth, where is lower end of grid-form deep cement mixing walls, were almost same behaviour. The peak compressive axial forces of pile of 1.0m diameter were about 690kN at pile head and 760kN at intermediate depth, respectively, and the peak bending moments of the pile were about 210kNm at pile head and 155kNm at intermediate depth, respectively. It is estimated that the frictional resistances around the piles enclosed by the grid-form walls were small and also the bending moments at pile head were reduced by the grid-form walls whereas those at lower end of the grid-form walls behaved similar to those at pile head. In addition, the bending moments at the pile head and those at the intermediate depth increased during large deformation of the ground in spite that the inertial force of building was not significant.

REFERENCES

Hamada, J., Tsuchiya, T. and Yamashita, K. (2009): Theoretical equations to evaluate the stress of piles on piled raft foundation during earthquake, *J. Structural Const. Eng. (AIJ)*, **Vol. 74, No. 644**, 1759-1767 (in Japanese).

Hamada, J., Tsuchiya, T., Tanikawa, T. and Yamashita, K. (2011): Lateral loading tests on piled raft foundations at large scale and their analyses, *International Conference on Advances in Geotechnical Engineering*, Nov.7-9, pp.1059-1064.

Horikoshi, K., Matsumoto, T., Hashizume, Y., Watanabe, T. and Fukuyama, H. (2003): Performance of piled raft foundations subjected to static horizontal loads, *International Journal of Physical Modelling in Geotechnics*, **3(2)**, 37-50.

Katzenbach, R., Arslan, U. and Moormann, C. (2000): Piled raft foundation projects in Germany, *Design applications of raft foundations*, **Hemsley J.A. Editor, Thomas Telford**, 323-392.

Katzenbach, R. and Turek, J. (2005): Combined pile-raft foundation subjected to lateral loads, *Proc. 16th Int. Conf. On Soil Mechanics and Geotechnical Engineering*, pp.2001-2004.

Kitiyodom, P. and Matsumoto, T. (2003): A simplified analysis method for piled raft foundations in non-homogeneous soils, *Int. J. Numer. Anal. Meth. Geomech*., pp85-109.

Mandolini, A., Russo, G. and Viggiani, C. (2005): Pile foundations: Experimental investigations, analysis and design, *Proc. 16th ICSMGE*, **Vol.1**, 177-213.

Matsumoto, T., Fukumura, K., Kitiyodom,P., Horikoshi, K. and Oki, A. (2004): "Experimental and analytical study on behaviour of model piled rafts in sand subjected to horizontal and moment loading", *International Journal of Physical Modeling in Geotechnics*, **4(3)**, 1-19.

Matsumoto, T., Nemoto, H., Mikami, H., Yaegashi, K., Arai, T. and Kitiyodom, P. (2010): Load tests of piled raft models with different pile head connection conditions and their analyses, *Soils and Foundations*, **Vol.50, No.50**, 63-81.

Mendoza, M. J., Romo, M.P., Orozco, M. and Dominguez, L. (2000): Static and seismic behavior of a friction pile-box foundation in Mexico City clay, *Soils & Foundations*, **Vol.40, No.4**, 143-154.

Poulos, H.G. (2001): Piled raft foundations: design and applications, *Geotechnique* 51, **No.2**, 95-113.

Watanabe,T., Fukuyama,H., Horikoshi,K. and Matsumoto,T (2001): Centrifuge modeling of piled raft foundations subjected to horizontal loads, *Proc. 5th Int. Conf. On Deep Foundation Practice incorporating Piletalk Int.*, pp. 371-378.

Yamashita, K., Yamada, T. and Hamada, J. (2011a): Investigation of settlement and load sharing on piled rafts by monitoring full-scale structures, *Soils & Foundations*, **Vol.51, No.3**, 513-532.

Yamashita, K., Hamada, J. and Yamada, T. (2011b): Field measurements on piled rafts with grid-form deep mixing walls on soft ground, *Geotechnical Engineering Journal of the SEAGS & AGSSEA*, **Vol.42, No.2**, 1-10.

Yamashita, K., Hamada, J., Onimaru, S. and Higashino, M. (2012): Seismic behavior of piled raft with ground improvement supporting a base-isolated building on soft ground in Tokyo, *Soils & Foundations*, **Vol.52, No.5**, the Special Issue for the 2011 off the Pacific coast of Tohoku Earthquake (accepted for publication).